Isobaric Vapor–Liquid Equilibria of Ethyl Acetate + Ethanol Mixtures at 760 ± 0.5 mmHg

Juan Ortega* and Juan A. Peña

Cátedra de Termodinámica y Físicoquímica, Escuela Superior de Ingenieros Industriales de Las Palmas, Canary Islands, Spain

Casiano de Alfonso

Unidad de Tribología e Ingeniería Química del Instituto Rocasolano, C.S.I.C., Madrid, Spain

New isobaric vapor–liquid equilibrium data of the system ethyl acetate + ethanol at 760 ± 0.5 mmHg, measured in a small-capacity recirculating still, are presented. In the thermodynamic treatment of the data, the vapor phase is considered nonideal. This system presents an azeotrope at 71.7 °C with a composition of 0.519 mol % in ethyl acetate. The data were correlated with different equations, the parameters of which are calculated and reported.

Introduction

The isobaric vapor–liquid equilibrium data of ethyl acetate with ethanol have been reported by many authors (*1–8*). Nonetheless, we decided to carry out this study in a continuation of the research on the thermodynamic properties of the systems esters + alkanols conducted in our department. As well as contributing to our present knowledge of this system, the experimental data obtained will serve to confirm the applicability and accuracy of a new small-capacity recirculating still.

The results of the measurements of the isobaric vapor–liquid equilibria, recorded at 760 ± 0.5 mmHg, of the system ethyl acetate + ethanol were treated thermodynamically considering the nonideality of the vapor phase, the values of the compositions of both phases and the activity factors being compared with those available in the literature. In the correlation of the experimental data the classic equations of Redlich–Kister, Margüles, and Van Laar were used, as well as the models suggested by Wilson and Renon and Prausnitz (NRTL) and the modified equation of Abrams and Prausnitz (UNIQUAC), and an equation proposed by one of us (*9*) that is applied for the first time in the correlation of vapor–liquid equilibrium data.

Experimental Section

Chemicals. Both the ethanol (puriss p.a. > 99.8 mol %) and the ethyl acetate (puriss p.a. > 99.5 mol %) were supplied by Fluka and used without further purification. However, both products were degassed and dried with a molecular sieve (Union Carbide, Type A4, by Fluka), the density, refractive index, and boiling point of the components given in Table I being seen to be in quite good agreement with those found in the literature.

Apparatus and Procedure. The apparatus used in this work was the type that recirculates both phases, with a charge capacity of some 50 cm^3. A diagram is provided in Figure 1.

Boiling of the liquid phase was achieved by means of stabilized electric heating in the double-walled inverted glass container A, which is fed from the main chamber by the recirculating liquid phase and condensed vapor. A tube, B, acting as a Cottrell pump, through which a mixture of liquid and vapor ascends from the boiling liquid mixture in A, protrudes from the top of the boiling vessel A. This allows the boiling temperature to be observed and also prevents reheating of the liquid over a wide vaporization interval of the solution. A probe inserted into the outlet of the Cottrell pump at T_1 marks the boiling temperature, and is shielded by tube C which reduces the possibility of drops of liquids being carried off with the vapor phase as it passes through the connecting tube to the coolant H. The liquid dripping from the probe and the adjacent walls falls into the funnel E and thence to the receiver F, with a volume of 3.5 cm^3, to return via C to the inverted glass container A. The constriction in the tube connecting G to A prevents the boiling mixture from passing back due to the fluctuations caused during the process of formation of the vapor bubbles. However, as an additional precaution, the tube G was filled with Raschig rings. The vapor reaches the coolant J where it condenses upon contact with the cold water circulating there, and the condensate is collected at L. The vaporization state of the mixture can be observed and controlled by means of the drop counter K. The bottom of the condenser J is connected to pressure equipment, which is described later.

In order to prevent vapor condensation in the main chamber this part of the apparatus is lagged with asbestos and glass wool, and an electric resistance is installed at D. The effect of this element is verified with a second probe at T_2. The interval of temperature $\Delta t = t_2 - t_1$ must be considered, since for $\Delta t < 0$ °C partial condensation of the vapor phase takes place, it being found that true equilibrium states are achieved when it is verified.

$$0.5\ °C \leq \Delta t \leq 1\ °C \qquad (1)$$

The lateral outlets M_L and M_V, equipped with threaded stoppers with silicone septa, are used for sampling the liquid and vapor, respectively. Samples are obtained with hypodermic syringes which are cooled externally under refrigeration in order to cool the extracted solutions rapidly.

Two Teflon stopcocks, LI_1 and LI_2, permit drainage of unusable solution whenever necessary. This operation is normally carried out only after the series of experiments has ended, since new fresh product can also be added by injection at M_L.

Since atmospheric pressure at our place of work is slightly over 760 mmHg, it was considered necessary to connect the equipment to a vacuum pump, thus obtaining a constant pressure with a better accuracy of ±0.5 mmHg. The system is comprised of a small-power vacuum pump connected to a Vakuumat electronic instrument by Normschliff Gerâteban Wertheim. By means of an electronically controlled valve, this apparatus corrects the variations in pressure existing between the equilibrium still and the required pressure. This pressure is indicated by a manometer connected at the outlet of the electronic system. A steel receiving vessel is placed both at the pump outlet and at the entrance to the equilibrium vessel in order to lessen the small oscillations in pressure. Before beginning with the selected mixture, data were obtained for the mixture ethanol + water, a deviation lower than 1% being

0021-9568/86/1731-0339$01.50/0

Table I. Physical Constants of the Pure Compounds at Atmospheric Pressure

compd	n_D(298.15 K) expt	n_D(298.15 K) lit.	ρ(298.15), kg·m^{-3} expt	ρ(298.15), kg·m^{-3} lit.	bp, K expt	bp, K lit.
ethyl acetate	1.3699	1.36979 (*10*)	894.34	894.55 (*10*)	350.3	350.26 (*10*)
		1.3728 (*11*)		894.6 (*11*)		350.30 (*11*)
ethanol	1.3594	1.35944 (*10*)	785.05	785.04 (*10*)	351.6	351.44 (*10*)
		1.35929 (*11*)		785.08 (*11*)		351.50 (*11*)

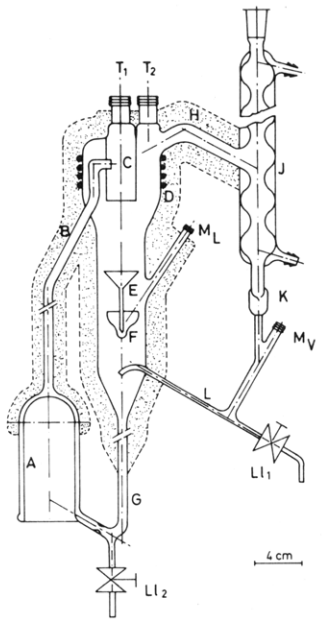

Figure 1. Schematic diagram of experimental equipment: A, inverted boiling flask; B, Cottrell pump; C, vapor tube; D, electric heater; E, funnel; F, receiver for collecting phase liquid; G, returning condensate; H, vapor tube J, cooler; K, drop counter; LI_1 and LI_2, cocks; M_L and M_V, sampling of liquid and vapor phase; T_1 and T_2, thermometers.

observed with respect to the data given in ref *12*. The temperatures T_1 and T_2, with an accuracy of ±0.1 °C, were obtained on a three-channel digital instrument by Bailey Instruments, previously calibrated according to IPTS-68 indications.

Upon cooling of the samples collected from the liquid and vapor phases, their respective compositions were determined by densimetric analysis, using a digital densimeter by Anton Paar, Model DMA-55 and following a technique described in a previous work (*13*). Prior to this, the calibration curves for ethyl acetate + ethanol were determined at 298.15 ± 0.01 K, the regular distribution of the V_m^E being observed, which values will be published later elsewhere. The error observed in the determination of the compositions of both phases was lower than 2×10^{-4}.

Results and Discussion

The vapor–liquid equilibrium data at 760 ± 0.5 mmHg are given in Table II, while the curve ($y - x$) vs. x appears in Figure 2, allowing better comparison with existing literature data. It is interesting to note that the mixture ethyl acetate (1) + ethanol (2) formed an azeotrope at a molar concentration of $x_1 = y_1 = 0.519$ and at $t = 71.7$ °C. The references cited in this article present the following values for the azeotrope: $x_1 = 0.52$ (*1*); 0.57 (*2*); 0.547 (*3*); 0.54 (*4*); 0.559 (*5*); 0.54 (*6*); 0.559 (*7*); 0.531 (*8*); and t (°C) = 71.8 (*1*); 72.1 (*2*); 72.1 (*3*); 71.8 (*4*); 71.7 (*5*); 72.2 (*6*); 71.7 (*7*); 71.7 (*8*), a good agreement being observed between the azeotropic temperature given by us and that cited in some references; however, a greater discrepancy exists in the concentration. The clearest comparison of the composition in equilibrium appears in Figure 2.

Table II. Experimental Vapor–Liquid Equilibrium Data for the System Ethyl Acetate–Ethanol at 760 ± 0.5 mmHg

t, °C	x	y	γ_1	γ_2
77.4	0.0248	0.0577	2.302	1.001
77.2	0.0308	0.0706	2.282	1.001
76.8	0.0468	0.1007	2.170	1.001
76.6	0.0535	0.1114	2.113	1.004
76.4	0.0615	0.1245	2.067	1.005
76.2	0.0691	0.1391	2.069	1.004
76.1	0.0734	0.1447	2.032	1.006
75.9	0.0848	0.1633	1.998	1.004
75.6	0.1005	0.1868	1.947	1.005
75.4	0.1093	0.1971	1.901	1.010
75.1	0.1216	0.2138	1.871	1.015
75.0	0.1291	0.2234	1.848	1.015
74.8	0.1437	0.2402	1.796	1.018
74.7	0.1468	0.2447	1.797	1.019
74.5	0.1606	0.2620	1.770	1.020
74.3	0.1688	0.2712	1.754	1.026
74.2	0.1741	0.2780	1.749	1.027
74.1	0.1796	0.2836	1.735	1.030
74.0	0.1992	0.3036	1.680	1.029
73.8	0.2098	0.3143	1.662	1.035
73.7	0.2188	0.3234	1.645	1.037
73.3	0.2497	0.3517	1.589	1.052
73.0	0.2786	0.3781	1.546	1.062
72.7	0.3086	0.4002	1.491	1.081
72.4	0.3377	0.4221	1.452	1.101
72.3	0.3554	0.4331	1.420	1.114
72.0	0.4019	0.4611	1.350	1.155
71.9_5	0.4184	0.4691	1.321	1.173
71.9	0.4244	0.4730	1.316	1.179
71.8_5	0.4470	0.4870	1.288	1.196
71.8	0.4651	0.4934	1.256	1.224
71.7_5	0.4755	0.4995	1.246	1.236
71.7	0.5100	0.5109	1.190	1.295
71.7	0.5669	0.5312	1.113	1.405
71.7_5	0.5965	0.5452	1.084	1.460
71.8	0.6211	0.5652	1.078	1.483
71.9	0.6425	0.5831	1.071	1.501
72.0	0.6695	0.6040	1.061	1.536
72.1	0.6854	0.6169	1.055	1.555
72.3	0.7192	0.6475	1.049	1.590
72.5	0.7451	0.6725	1.045	1.614
72.8	0.7767	0.7020	1.036	1.657
73.0	0.7973	0.7227	1.032	1.685
73.2	0.8194	0.7449	1.029	1.726
73.5	0.8398	1.7661	1.022	1.763
73.7	0.8503	0.7773	1.018	1.782
73.9	0.8634	0.7914	1.014	1.815
74.1	0.8790	0.8074	1.010	1.877
74.3	0.8916	0.8216	1.006	1.925
74.7	0.9154	0.8504	1.002	2.036
75.1	0.9367	0.8798	1.000	2.152
75.3	0.9445	0.8919	0.999	2.190
75.5	0.9526	0.9038	0.997	2.264
75.7	0.9634	0.9208	0.998	2.396
76.0	0.9748	0.9348	0.992	2.831
76.2	0.9843	0.9526	0.995	3.278
76.4	0.9903	0.9686	0.999	3.487

The activity coefficients of the liquid phase were calculated by means of eq 2 and presented slight deviations from ideality.

$$\gamma_i = (y_i p / x_i p_i^0) \exp\left[\frac{(B_{ii} - V_i^0)(p - p_i^0) + (1 - y_i)^2 p \delta_{ij}}{RT}\right] \quad (2)$$

where

$$\delta_{ij} = 2B_{ij} - B_{ii} - B_{jj} \quad (3)$$

The pure components' vapor pressures were calculated by using the Antoine equation, with the constants reported in ref *14*. The second virial coefficients were estimated by the Pitzer correlation, modified by Prausnitz (*15*) for mixtures. Considering the closeness of the boiling points of ethyl acetate (77.15 °C) and of ethanol (78.35 °C), and the consequently small value of the dT/dx slope, the corresponding enthalpies of mixture have been disregarded. Thus, the consistency test proposed by Herington (*16*) was applied, giving $D - J < 3\%$. The correlation of results was performed by using the Redlich–Kister, Margüles, and Van Laar equations and the models proposed by Wilson, by Renon and Prausnitz (NRTL), and by Abrams and Prausnitz (UNIQUAC), the parameters of which were decided by fitting the Q function $= g^E/RT$. The coefficients of the respective equation appear in Table III together with the standard deviations obtained for each case. The parameters of the first three equations were obtained by a least-squares method, while an appropriate algorithm for nonlinear functions (*17*) was used for the remainder.

In an earlier work (*9*), the use of a polynomial equation in Z was recommended, in order to fit the excess thermodynamic functions. For application to the vapor–liquid equilibrium data, the said equation is expressed as follows

$$Q = g^E/RT = x(1 - x)\sum_{l}^{n} A_{l-1}Z^{l-1} \quad (4)$$

where

$$Z = x/[x + K(1 - x)] \quad (5)$$

The values of the coefficients A_{l-1} were determined by a least-squares method (applying an F test), while K was estimated by optimization with a view to achieving the smallest deviation of the Q values. These coefficients are given in Table III, where it is found that the best correlation of the experimental data corresponds to the equation proposed in this work. Thus, henceforward this equation was employed to fit $(y - x)$ vs. x as well as to determine the ln γ_i. The curve drawn in Figure 2 gave a standard deviation of the experimental data of 7.2×10^{-3}. The individual activity coefficients were obtained by means of the relationships

$$\ln \gamma_1 = Q + (1 - x)\frac{dQ}{dx} \quad (6)$$

$$\ln \gamma_2 = Q - x\frac{dQ}{dx} \quad (7)$$

For the equation proposed (*4*), these values are

$$\ln \gamma_1 = x_2^2\left[\sum_{l}^{n} A_{l-1}Z^{l-1} + x_1K\left(\frac{Z}{x_1}\right)^2\sum_{l}^{2n-1} lA_lZ^{l-1}\right] \quad (8)$$

$$\ln \gamma_2 = x_1^2\left[\sum_{l}^{n} A_{l-1}Z^{l-1} - x_2K\left(\frac{Z}{x_1}\right)^2\sum_{l}^{2n-1} lA_lZ^{l-1}\right] \quad (9)$$

where Z is related to the composition through (5). The generic index $i = 1, 2, 3, \ldots, n$, has as maximum value the degree of the polynomial achieved for eq 4, when it is applied to the corresponding binary system. The values of ln γ_1, ln γ_2, and ln (γ_1/γ_2) were determined by using these equations; comparison of these values with those determined from the experimental data caused, respectively, deviations of 0.03, 0.09, and 0.10. From eq 8 and 9, the activities at infinite dilution can be estimated by way of ln $\gamma_1^\infty = A_0$ and ln $\gamma_2^\infty = \sum A_{l-1}$. The results obtained, together with those from the literature, were $\gamma_1^\infty = 2.78$ [3.83 (*1*); 2.50 (*2*); 2.34 (*3*); 2.34 (*4*); 2.36 (*5*); 2.56 (*6*); 2.24 (*7*); 2.72 (*8*)], $\gamma_2^\infty = 2.15$ [2.18 (*1*); 2.17 (*2*); 2.22 (*3*); 2.11 (*4*); 2.19 (*5*); 1.94 (*6*); 2.34 (*7*); 2.17 (8)].

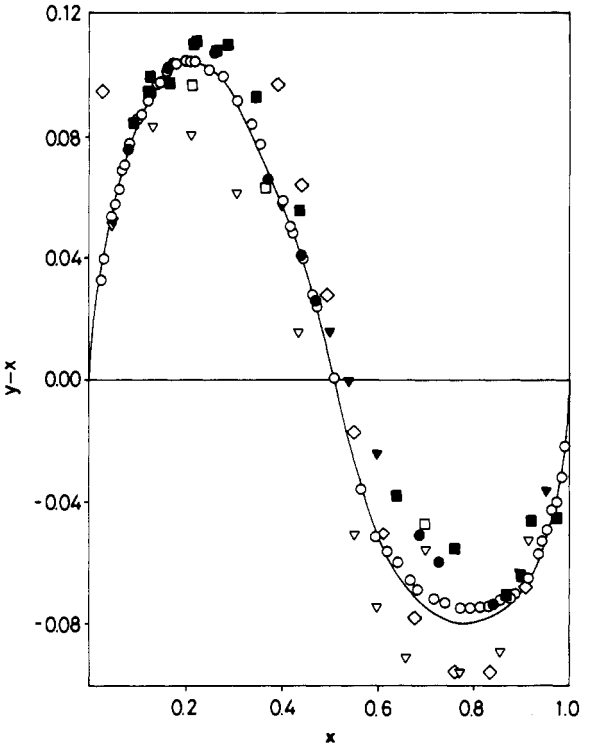

Figure 2. Plot of $(y - x)$ as a function of composition of ethyl acetate at 760 ± 0.5 mmHg and some data derived from literature: (◇) ref *1*; (■) ref *2*; (●) ref *3*; (▼) ref *4*; (□) ref *5*; (▽) ref *6*; (○) our experimental values. In order to avoid confusion we have not presented the values corresponding to ref *7* and *8*.

Table III. Fitting Parameters and Standard Deviations, $\sigma(Q)$, of the Q Function for the System Ethyl Acetate–Ethanol at 760 ± 0.5 mmHg

method	parameters	$\sigma(g^E/RT)$
Redlich–Kister	$A_0 = 0.8487$, $A_1 = 0.0214$, $A_2 = -0.0824$, $A_3 = -0.0192$	0.0025
Margüles	$A_{12} = 0.8335$, $A_{21} = 0.8300$	0.0037
Van Laar	$A_{12} = 0.8347$, $A_{21} = 0.8236$	0.0037
Wilson	$\Lambda_{12} = 0.6125$, $\Lambda_{21} = 0.6374$[a]	0.0040
NRTL ($\alpha = 0.47$)	$\tau_{12} = 0.4461$, $\tau_{21} = 0.4877$[b]	0.0039
UNIQUAC ($z = 10$)	$\tau_{12} = 0.5247$, $\tau_{21} = 1.1758$[c]	0.0037
eq 4	$A_0 = 1.0241$, $A_1 = 1.4187$, $A_2 = 2.8797$, $A_3 = -1.7206$, $K = 0.269$	0.0019

[a] $\Lambda_{ij} = (v_j^L/V_i^L)\exp\{-[(\lambda_{ij} - \lambda_{ii})/RT]\}$. [b] $\tau_{ji} = (g_{ji} - g_{ii})/RT$. [c] $\tau_{ji} = \exp[-(u_{ji} - u_{ii})/RT]$.

In further works, the efficiency of this small-capacity recirculating still and the usefulness of the relationships presented here for different binary systems corresponding to different homologous families of esters and alkanols will be verified.

Registry No. Ethanol, 64-17-5; ethyl acetate, 141-78-6.

Literature Cited

(1) Kireev, V. A.; Klinov, I. Y.; Grigororich, A. N. *Khim. Mashinostr. (Moscow)* **1936** *5*, 34.
(2) Murti, P. S.; Van Winkle, M. *Chem. Eng. Data Ser.* **1958**, *3*, 72.
(3) Griswold, J.; Chu, P. L.; Winsaner, W. O. *Ind. Eng. Chem.* **1949**, *41*, 2352.
(4) Chu, J. C.; Getty, R. J.; Breennecke, L. F.; Paul, R. *Distillation Equilibrium Data*; New York, 1950.
(5) Babich, S. V.; Borozdina, I. V.; Kushner, T. M.; Serafimov, L. A. *Zh. Prikl. Khim.* **1968**, *41*, 589.
(6) Van Zandijcke, F.; Verhoeye, L. *J. Appl. Chem. Biotechnol.* **1974**, *24*, 709.
(7) Furnas, C. C.; Leighton, W. B. *Ind. Eng. Chem.* **1937**, *29*, 709.
(8) Kato, M.; Konishi, H.; Hirata, M. *J. Chem. Eng. Data* **1970**, *15*, 435.
(9) Ortega, J. *J. Chem. Eng. Data* **1985**, *30*, 465.

(10) Riddick, J. A.; Bunger, W. B. *Techniques of Chemistry*; Wiley-Interscience: New York, 1970; Vol II.
(11) Timmermans, J. *Physico-Chemical Constants of Pure Organic Compounds*; Elsevier: Amsterdam, 1965.
(12) Paul, R. N. *J. Chem. Eng. Data* **1976**, *21*, 165.
(13) Ortega, J.; Peña, J. A.; Paz-Andrade, M. I.; Pintos, M.; Romani, L. *J. Chem. Thermodyn.* **1985**, *17*, 321.
(14) Boublik, T.; Fried, V.; Hála, E. *The Vapour Pressures of Pure Substances*; Elsevier: New York, 1973.
(15) Prausnitz, J. M. *Molecular Thermodynamics of Fluid-Phase Equilibria*, Prentice-Hall: Englewood Cliffs, NJ, 1969.
(16) Herington, E. F. G. *J. Inst. Pet.* **1951**, *37*, 457.
(17) Marquardt, D. W. *J. Soc. Ind. Appl. Math.* **1963**, *11*, 431.

Received for review August 12, 1985. Revised manuscript received January 29, 1986. Accepted March 21, 1986.

Surface Tension and Density of the Molten KCl–LiCl and $PbCl_2$–KCl–LiCl Systems

Guankun Liu, Torstein Utigard, and James M. Toguri*

Department of Metallurgy and Materials Science, University of Toronto, Toronto, Ontario, Canada M5S-1A4

The maximum bubble pressure method was used to determine the surface tension and density of melts within the binary KCl–LiCl and the ternary $PbCl_2$–KCl–LiCl systems. The temperature range of this study was from 723 to 1173 K. In all cases, the surface tension was found to decrease with increasing temperature. In the ternary system at constant molar ratios of KCl to LiCl, a minimum in the surface tension was observed at approximately 45 mol % $PbCl_2$. The ternary surface tension values were found to obey this simple additivity expression of the binary surface tensions of KCl–LiCl and KCl–$PbCl_2$. Based on these findings, constant surface tension contours have been evaluated. The density obtained in the present study agree well with the previously determined densities obtained by using a bottom-balance Archimedean technique reported by this laboratory.

Introduction

The present process for the extraction of lead from lead sulfide concentrates gives rise to problems with respect to environmental concerns. In anticipation of strict legislation controlling the emissions of heavy metals as well as sulfur dioxide, new processes have been proposed. One such process is the conversion of lead sulfide to a chloride followed by fused-salt electrolysis to produce metallic lead and chlorine (*1–3*). The chlorine produced is recycled directly or indirectly for the production of lead chloride.

Lead chloride alone is not a good electrolyte because it has a high vapor pressure and exhibits poor current efficiency with respect to lead production. Both the $PbCl_2$–KCl–LiCl and $PbCl_2$–KCl–NaCl ternary systems have been suggested as possible electrolytes due to their suitable physical properties. The $PbCl_2$–KCl–LiCl system has a higher molar conductivity, but due to the hygroscopic nature of LiCl, the $PbCl_2$–KCl–NaCl ternary system has been suggested as an alternative electrolyte.

Recently, the surface tensions of melts in the $PbCl_2$–KCl–NaCl ternary system were determined in this laboratory (*4*). As a continuation of this work, the surface tension of the molten salt system $PbCl_2$–KCl–LiCl as a function of composition and temperature in the range of interest for the electrolytic process of lead recovery was studied. For the determination of the ternary system, reliable data on the binary KCl–LiCl were not available. Consequently, the surface tension of the binary KCl–LiCl was also measured.

Experimental Section

The experimental apparatus and procedure adopted for the present study have been described in detail previously (*4*) and thus only a brief description is given here. The well established maximum bubble pressure technique was selected for the determination of the surface tension and density. It involves the slow formation of a gas bubble at the tip of a capillary immersed in the molten salt. Simultaneously, the pressure of the gas used to form the bubble is measured in order to determine the maximum pressure developed inside the bubble at the very instant it bursts. Schrödinger (*5*) developed the following relationship between the surface tension and the maximum bubble pressure.

$$\gamma = \frac{rP_\gamma}{2}\left[1 - \frac{2}{3}\left(\frac{r\rho g}{P_\gamma}\right) - \frac{1}{6}\left(\frac{r\rho g}{P_\gamma}\right)^2\right] \qquad (1)$$

γ is the surface tension, r is the radius of the capillary, P_γ is the maximum pressure difference inside and outside the bubble at the capillary tip, ρ is the density difference between the liquid salt and the gas, and g is the acceleration of gravity.

Apparatus. The overall apparatus used in this investigation is shown in Figure 1. The furnace had a uniform temperature (2.5 K) region of 5 cm. The salt mixtures were contained in graphite crucibles with an inner diameter of 26 mm and a height of 47 mm under a purified argon atmosphere. The quartz capillary tubes were 5 cm long, with an outer diameter of about 2.1 mm and with an inner diameter of about 1.03 mm.

Procedure. The potassium chloride (Fisher A.C.S. grade), the lithium chloride (CERAC, 99.8%), and the lead chloride (Baker Analysed reagent grade) were stored and handled in a drybox filled with a dry argon atmosphere. The salts were predried in a vacuum oven at 423 K before mixing. A graphite crucible with the salt mixture was positioned inside the furnace which was flushed with argon and heated to the desired temperature. Excess pressure was applied to the capillary while it was lowered toward the melt surface. The capillary was then lowered very slowly until a sudden pressure jump was registered by the pressure transducer, indicating that the capillary had touched the melt surface and the surface position was recorded.

The bubbling rate was adjusted to about 1 bubble/min which was in the region where the transducer output was independent of the gas flow rate. The pressure was increased linearly with the immersion depth until a bubble was released at the capillary tip followed by a sudden decrease in the pressure. The capillary immersion depth was changed several times while the maxi-

0021-9568/86/1731-0342$01.50/0